Computational investigation of the external excitation frequency effect on liquid sloshing phenomenon

Abdallah Bouabidi *, Zied Driss, Nihed Cherif, Mohamed Salah Abid
Laboratory of Electro-Mechanic Systems (LASEM)
National School of Engineers of Sfax (ENIS)
B.P. 1173, km 3.5 Soukra, 3038 Sfax, TUNISIA
bouabidi_abdallah@yahoo.fr

Abstract: - In this work, the Computational Fluid Dynamic (CFD) method was used to simulate the liquid sloshing phenomenon in a rectangular tank. The tank was subjected to an external sinusoidal excitation. Particularly, we are interested on the study of the external excitation frequency effect. The hydrodynamic parameters describing the flow like the velocity field, the average velocity, the static and the dynamic pressure were presented. All numerical results were conducted using the commercial CFD code "FLUENT". The volume of fluid (VOF) method based on the finite volume method was used to simulate incompressible viscous two phase flow in a tank partially filled with liquid. The results show that the liquid sloshing significantly depends on the frequency value. For a weak value of frequency, the liquid moves slowly. With the increase of the frequency, the liquid sloshing becomes more violent. A good agreement has been shown by comparing our numerical results with the experimental one.

Key-Words: - External excitation, frequency, turbulent flow, finite volume method, VOF

1 Introduction

When a container partially filled with liquid is subjected to an external excitation, the phenomena of sloshing are present. These phenomena are interest of many engineering sections such as petroleum cylindrical tanks, road tankers, aerospace vehicles and liquefied natural gas carriers. Thus, the control of sloshing phenomena in different types of container is very important. In fact, the sloshing can causes structure problems. This phenomenon of liquid sloshing in the partially filled container is a result of different external excitations. Therefore, it has been studied for many excitation types. For example, Akyildiz et al. [1] developed an experimental setup to study the phenomena of sloshing in a rectangular tank subjected to an external sinusoidal excitation. They studied sloshing for different values of fill depth and the baffle effect. Molin et al. [2] investigated experimentally and numerically the phenomenon of sloshing in a tank excited with horizontal and rolling movement. Yan et al. [3] discussed experimentally the effect of lateral and longitudinal excitations on the sloshing of the liquid in a partially filled tank. Jin et al. [4] studied experimentally the effect of horizontal perforated plates with different values of frequency and amplitude of an external sinusoidal excitation. Their study revealed that the amplitude and the frequency of the external excitation affect the behavior of the sloshing. Also, they showed that the use of the perforated horizontal plate can significantly reduce the sloshing in the tank. Godarzi et al. [5] investigated numerically the motion of the liquid in a partially filled container subjected to harmonic and seismic excitations. Hou et al. [9] analyzed numerically the liquid sloshing phenomenon in a rectangular tank subjected to external excitations. The volume of fluid (VOF) and the dynamic mesh technique are used to predict the deformation of the free surface and to impose the external excitations respectively. They compared the effect a single excitation and the effect of multiple coupled excitations. They concluded that the sloshing is more important for the case of multiple coupled excitations and the case of the resonant frequency. Meziani et al. [11] studied the problem of sloshing in rectangular tank subjected to an external sinusoidal excitation in the vertical direction. The sloshing phenomenon is also studied in a tank subjected to a lateral sinusoidal movement by many researchers [6-8]. Akyıldız et al. [10] analyzed the sloshing phenomena in a tank subjected to rotational flow for different values of rolling frequencies.

Nowadays, The CFD (computational fluid dynamics) is used in several studies fields [12-15]. Especially, Yu el al. [16] used the CFD technique to study the effect of the geometry variations on the nozzle flow. They concluded that the flow is considerably affected by the geometry configuration

in the nozzle. Andersson at al. [17] investigated the free surface evolution in a reservoir during spilling using the CFD technique. Mnasri et al. [18] studied the free surface deformation caused by moving cylinders. They used the moving mesh technique to impose the cylinders motion and the VOF method to predict the evolution of the free surface. In the other hand, the CFD technique is used on the study of the sloshing phenomena by many researchers. For example, Sriram et al. [19] investigated the liquid sloshing phenomenon in a tank subjected to horizontal and vertical excitation using the CFD method. Godderidge et al. [20] analyzed the motion of the liquid in a rigid tank subjected to lateral movement using the CFD technique. Bouabidi et al. [21] investigated the motion of the liquid in a rectangular tank with the commercial software "Fluent" .They studied effect of the vertical baffle height. Their results showed that the sloshing phenomenon decrease with the increase of the baffle height. According to the literature review, it is clear that the study of external excitation parameters is very interesting.

In this paper, we are interested on the study of the liquid sloshing phenomenon in a rectangular tank subjected to an external sinusoidal excitation using the CFD technique. The VoF method is used to predict the free surface evolution. The external excitation frequency effect on the sloshing violence is studied and analyzed. The numerical results like the velocity field, the static pressure and dynamic pressure are presented and discussed.

2 Geometrical arrangement

The considered geometry is a rectangular tank as shown in figure 1. This geometrical arrangement is similar to Panigrahy [22] application. In fact, the geometry is defined by the length L=0.6 m and the height equal to H=0.6 m. The tank is partially filled with liquid with the height h=0.1 m.

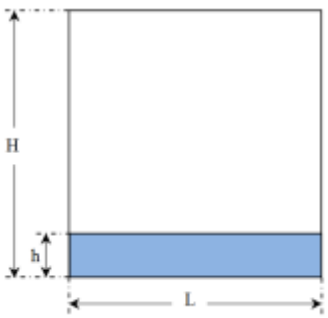

Fig. 1 Geometrical arrangement

3 Numerical model

3.1 Governing equations

The phenomenon of liquid sloshing in a rigid tank for an incompressible, immiscible fluid is governed by the continuity and the Navier-Stockes equations written as follows:

$$\frac{\partial \rho}{\partial t}+\frac{\partial}{\partial x_i}(\rho u_i)=0 \tag{1}$$

$$\frac{\partial}{\partial t}(\rho u_i)+\frac{\partial}{\partial x_j}(\rho u_i u_j)=-\frac{\partial p}{\partial x_i} + \frac{\partial}{\partial x_j}\mu\left(\frac{\partial u_i}{\partial x_j}+\frac{\partial u_j}{\partial x_i}\right)+F_i \tag{2}$$

Where u_i represent the velocity components, ρ represents the density, p represents the pressure, μ represents the viscosity and F_i is the external body force.

$$F_i=\rho g_j+\rho\frac{\partial^2 X}{\partial t^2} \tag{3}$$

The turbulence kinetic energy k and its dissipation rate ε are given by the following equations:

$$\frac{\partial}{\partial t}(\rho k)+\frac{\partial}{\partial x_i}(\rho k u_i)=\frac{\partial}{\partial x_j}\left[\left(\mu+\frac{\mu_t}{\sigma_k}\right)\frac{\partial k}{\partial x_j}\right] + G_k+G_b-\rho\varepsilon-Y_M+S_k \tag{4}$$

$$\frac{\partial}{\partial t}(\rho\varepsilon)+\frac{\partial}{\partial x_i}(\rho\varepsilon u_i)=\frac{\partial}{\partial x_j}\left[\left(\mu+\frac{\mu_t}{\sigma_\varepsilon}\right)\frac{\partial \varepsilon}{\partial x_j}\right] + C_{1\varepsilon}\frac{\varepsilon}{k}(G_k+C_{3\varepsilon}G_b)-C_{2\varepsilon}\rho\frac{\varepsilon^2}{k}+S_\varepsilon \tag{5}$$

G_k and G_b are the generation of turbulence kinetic energy ($kg.m^{-1}.s^{-3}$) respectively due to the mean velocity gradients and buoyancy. Y_M is the contribution of the fluctuating dilatation in compressible turbulence to the overall dissipation rate. The turbulent viscosity μ_t (Pa.s) is given by:

$$\mu_t=\rho C_\mu\frac{k^2}{\varepsilon} \tag{6}$$

The default values of the constants $C_{1\varepsilon}$, $C_{2\varepsilon}$, C_μ, σ_k and σ_ε are presented in table 1.

Table 1. Model constants

$C_{1\varepsilon}$	$C_{2\varepsilon}$	C_μ	σ_k	σ_ε
1.44	1.92	0.09	1.0	1.3

The external excitation is defined as follow:

$$X = A\sin(\omega t) \quad (7)$$

Where A and ω represents the amplitude and the frequency, respectively. The amplitude is fixed as A=0.1m for all simulation cases in this study.

According to Akyildiz et al. [23], the natural frequency is given by the following equation:

$$\omega_n = \sqrt{\frac{n\Pi g}{L}\tanh(\frac{n\Pi h}{L})} \quad (8)$$

Where L represents the length of the tank, h represents the liquid depth and n represents the mode number.

For the liquid sloshing phenomenon, the resonance frequency is different to the natural frequency of the fluid given by equation (8) for n=1 [23]. The natural frequency in this application is equal to f_p=0.79 Hz.

Four different values of frequency were studied (table 2).

Table 2. Frequency value

Frequency	Value (Hz)	Ratio f_i/f_p
f_1	0.25	0.31
f_2	0.5	0.63
f_3	0.79	1
f_4	0.9	1.14

The free surface is defined as the zero level set of a level-set function Φ given by the following equation:

$$\begin{aligned} \Phi(x_i, t) &> 0 \\ \Phi(x_i, t) &= 0 \\ \Phi(x_i, t) &< 0 \end{aligned} \quad (9)$$

The free surface evolution is given by the transport equation defined as follow:

$$\frac{\partial \Phi}{\partial t} + u_i \frac{\partial \Phi}{\partial x_i} = 0 \quad (10)$$

Where u_i represents the local velocity.

3.2 Numerical method

The commercial CFD code "Fluent" has been used to present the local flow characteristics in the tank. The VoF method (Volume of Fluid) is used to identify the two fluids; water and air. For the external excitation, a User Defined Function (UDF) is developed on language "C++" and interpreted in "Fluent".

The Navier-Stokes equations and the standard k-ε turbulence model equations were solved using a finite volume discretization method [24-25].

4 Numerical results and discussions

In this section, we presented the numerical results described the turbulent flow: the free surface evolution, the velocity fields, the average velocity, and the distribution of the static and the dynamic pressure. The numerical results are presented for four different values equals to f_1=0.25 Hz, f_2=0.5 Hz, f_3=0.79 Hz and f_4=0.9 Hz. For each frequency, the hydrodynamics parameters are given over time: at t=T/4, t=T/2, t=3T/4 and t=T.

4.1 Free surface evolution

The free surface elevation for the different values of frequency is presented at t=T/4, t=T/2, t=3T/4 and t=T as shown in figures 2, 3, 4 and 5 respectively. Globally, we note that the liquid moves in the same sense of the external excitation. In fact, at t=T/4 and t=T/2 the liquid moves from the right to the left for the different values of the frequency. At t=3T/4 and t=T, the liquid changes the movement sense and moves from the left to the right. In the other hand, such results indicate that the sloshing behaviour strongly depends on the frequency value. Indeed, the minimum motion of liquid is observed for the minimum value of frequency equal to f_1=0.25 Hz, whereas for the maximum sloshing has been observed for the frequency value equal to f_4=0.9 Hz. For f_1=0.25 Hz, the minimum free surface deformation has been observed for the different instances. The sloshing increases for f_2=0.5 Hz. For the natural frequency f_3=0.79 Hz, the movement of the liquid is more important than for f_1=0.25 Hz and f_2=0.5 Hz and lower than for f_4=0.9 Hz.

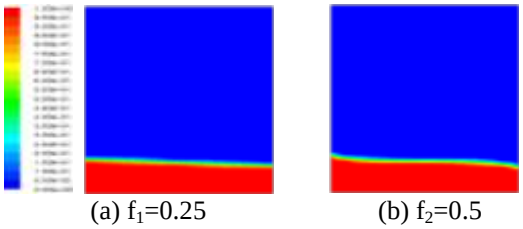

(a) f_1=0.25 (b) f_2=0.5

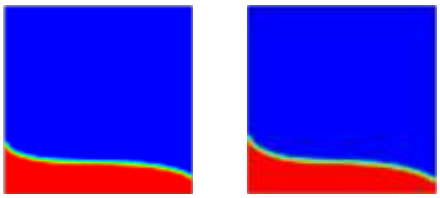

(c) f_3=0.79 (d) f_4=0.9

Fig. 2 Free surface evolution at t=T/4.

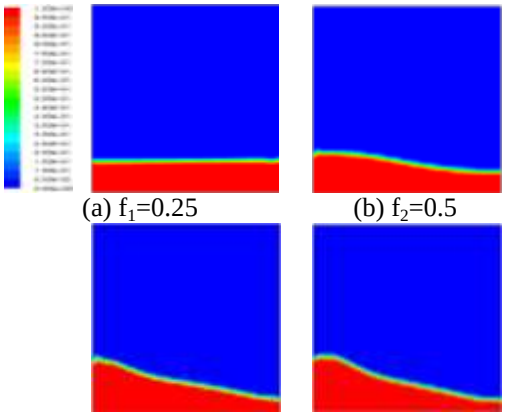

(a) f_1=0.25 (b) f_2=0.5

(c) f_3=0.79 (d) f_4=0.9

Fig. 3 Free surface evolution at t=T/2

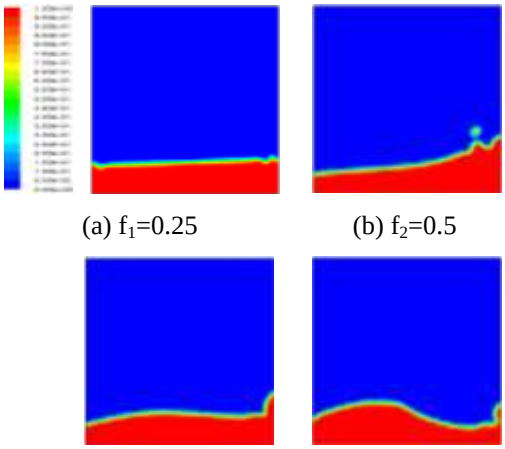

(a) f_1=0.25 (b) f_2=0.5

(c) f_3=0.79 (d) f_4=0.9

Fig. 4 Free surface evolution at t=3T/4.

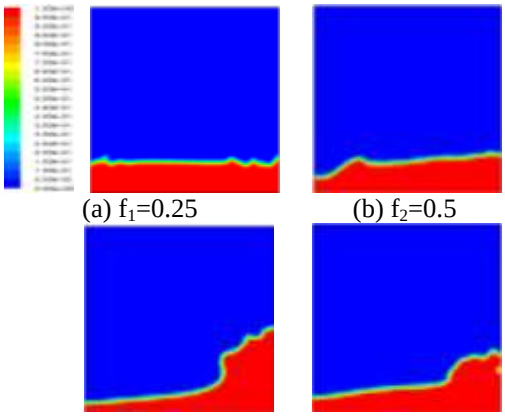

(a) f_1=0.25 (b) f_2=0.5

(c) f_3=0.79 (d) f_4=0.9

Fig. 5 Free surface evolution at t=T.

4.2 Velocity fields

The velocity field for the different values of frequency is shown in figures 6, 7, 8 and 9 for the different instances considered in this study. Globally, we note that the liquid motion creates a recirculation zones in the tank. In fact, for the f1 frequency a small recirculation zone appeared at t=T/4. In this case, the maximum value can be observed on the free surface close to the left wall. However, the velocity is near zero in the rest of the tank which means that liquid motion is very weak. At t=T/2, the recirculation zone appeared on the free surface close to the right wall. The maximum value of the velocity appeared in the recirculation zone. Also, we note that the velocity is different to zero closes the left wall on the free surface. At t=3T/4, the recirculation zones are more important. At t= T, many recirculation zones appear on the free surface close to the left and the right wall. In the other hand, we note that the highest value is observed at t=T, whereas the lowest value is observed at t=T/2. For the second value of frequency f_2=0.5 Hz, at t=T/4 the velocity value is more important in the bottom of the tank. Also, we note that a large recirculation is observed on the free surface. At t=T/2, the highest value has been observed on the free surface close to the wall. Two recirculation zones on the free surface close to the left wall appear at t=3T/4. At t=T, a recirculation zone appears close to the left and the right wall on the free surface of the liquid. For the natural frequency f_3=0.79 Hz, a large recirculation zone appears on the free surface in the center of the tank, whereas a small recirculation zone appears close to the left wall at T/4. At t=T/2, the liquid motion is more important. Three recirculation zones appear. Indeed, the first one is located in the center of the tank, the second appear close the left wall and the third appear in the right corner in the bottom of the tank. The highest value is observed in the bottom of the tank. At t=3T/4, one zone of recirculation is observed on the free surface. At t=T, two recirculation zones appear. The first is located in the right half of the tank where the maximum value is noted. For f_4=0.9 Hz, the behavior of the velocity is similar to the case of f_3=0.79 Hz at t=T/4. At t=T/2, the highest value is observed on the free surface close to the left wall. Three recirculation zones have been observed. At t=3T/4, a large recirculation zone is located on the free surface. At t=T, two small recirculation zones have been observed. From such results, we conclude that the velocity field depends strongly on the external excitation frequency. Also, such results indicate that the velocity field varies over time. In

fact, for each value of frequency the velocity evaluate over time.

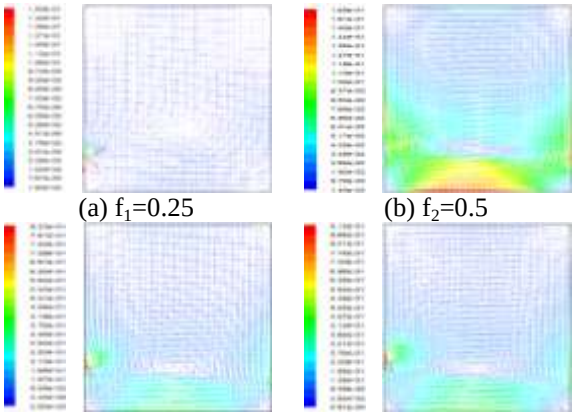

(a) f_1=0.25 (b) f_2=0.5

(c) f_3=0.79 (d) f_4=0.9

Fig. 6 Velocity field at t=T/4.

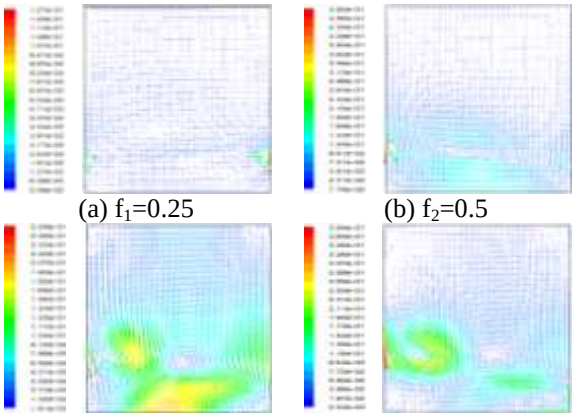

(a) f_1=0.25 (b) f_2=0.5

(c) f_3=0.79 (d) f_4=0.9

Fig. 7 Velocity field at t=T/2.

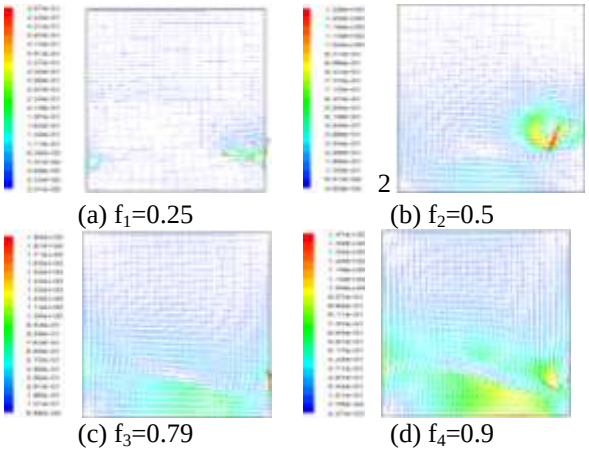

(a) f_1=0.25 2 (b) f_2=0.5

(c) f_3=0.79 (d) f_4=0.9

Fig. 8 Velocity field at t=3T/4.

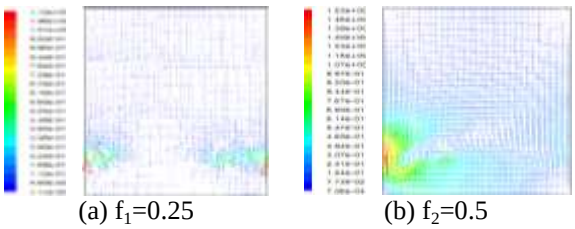

(a) f_1=0.25 (b) f_2=0.5

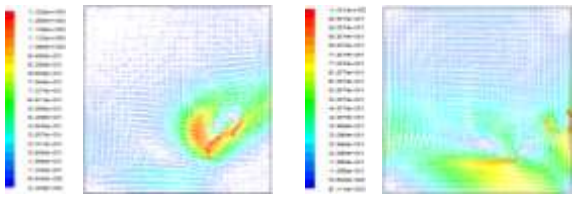

(c) f_3=0.79 (d) f_4=0.9

Fig. 9 Velocity field at t=T.

4. 3 Magnitude velocity

The distribution of the Magnitude velocity caused by the motion of the liquid in the tank for different values of frequency is shown in figures 10, 11, 12 and 13. Such results indicate that the distribution of the Magnitude velocity depends on the external excitation frequency. In fact, at t=T/4 the value of the average velocity increases with increase of the frequency. At this instant, the maximum value has been noted for f_4=0.9 Hz, whereas the minimum value can be observed for f_1=0.25 Hz. At t=T/2 and t=T, the liquid return to change the sense due to the change of the external excitation sense. Therefore, the maximum value can be observed for f_2=0.5 Hz at t=T/2 and for f_1=0.25 Hz at t=T. At t=3T/4, the maximum value is obtained for f_4=0.9 Hz. These results revealed that the location of the highest value of the mean velocity depends on the movement sense.

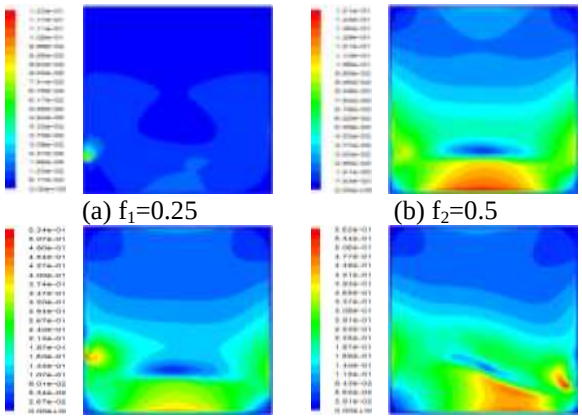

(a) f_1=0.25 (b) f_2=0.5

(c) f_3=79 (d) f_4=0.9

Fig. 10 Magnitude velocity at t=T/4.

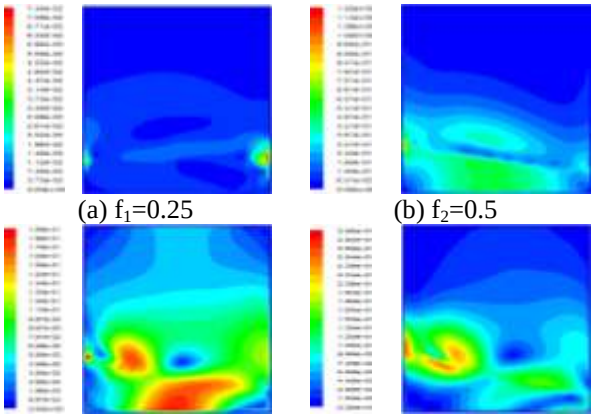

(a) f_1=0.25 (b) f_2=0.5

(c) f_3=0.79 (d) f_4=0.9

Fig. 11 Magnitude velocity at t=T/2.

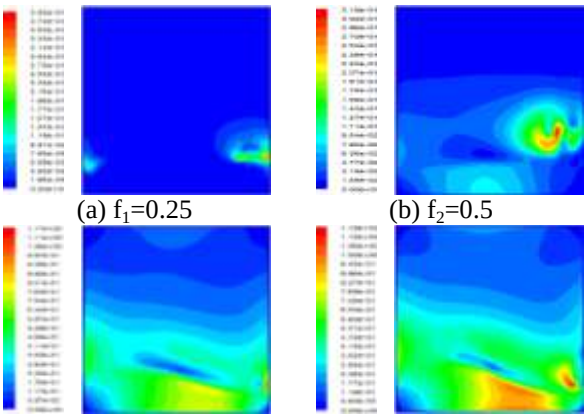

(a) f_1=0.25 (b) f_2=0.5

(c) f_3=0.79 (d) f_4=0.9

Fig. 12 Magnitude velocity at t=3T/4.

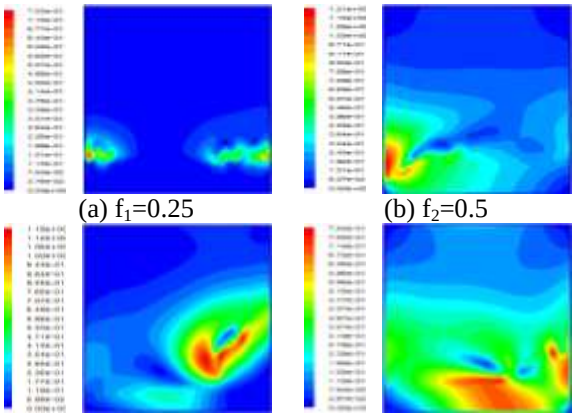

(a) f_1=0.25 (b) f_2=0.5

(c) f_3=0.79 (d) f_4=0.9

Fig. 13 Magnitude velocity at t=T.

4.4 Static pressure

Figures 14, 15, 16 and 17 show the distribution of the static pressure caused by liquid sloshing at different probes. From these results, we note that the location of the compression zones depends on the external excitation frequency value. Since the direction of movement of the fluid is the same during a half period, the location of the compression zones is the same one of the previous instant in a half period. In fact, at t=T/4 and t=T/2 the compression zones are located in the bottom of tank in the left corner, whereas it is located in the right corner at t=3T/4 and t=T. In the other hand, we note that the value of the static pressure increases with the increase of the movement frequency at t=3T/4 and t=T. Also, we note that the highest value of the static pressure is maximal for f_3=0.79 Hz At t=T/2 and t=3T/4.

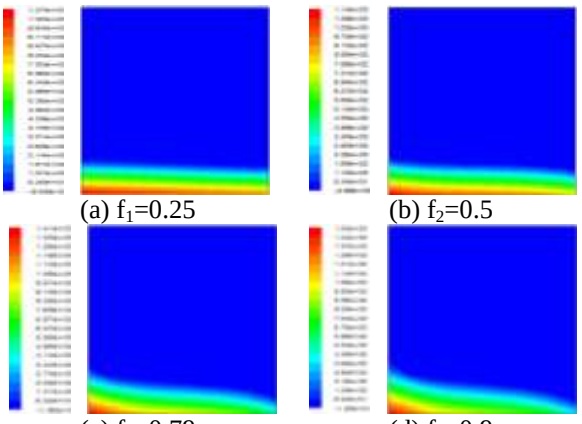

(a) f_1=0.25 (b) f_2=0.5

(c) f_3=0.79 (d) f_4=0.9

Fig. 14 Distribution of static pressure at t=T/4.

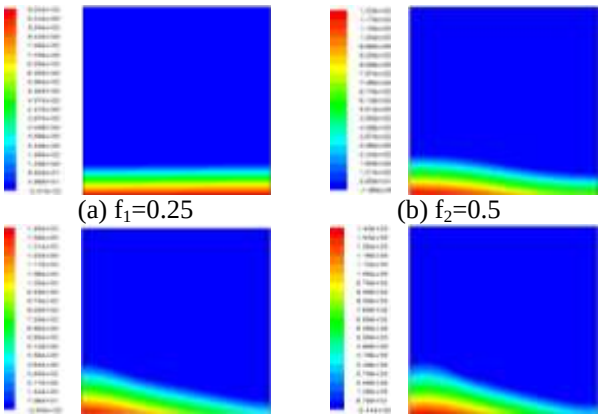

(a) f_1=0.25 (b) f_2=0.5

(c) f_3=0.79 (d) f_4=0.9

Fig. 15 Distribution of static pressure at t=T/2.

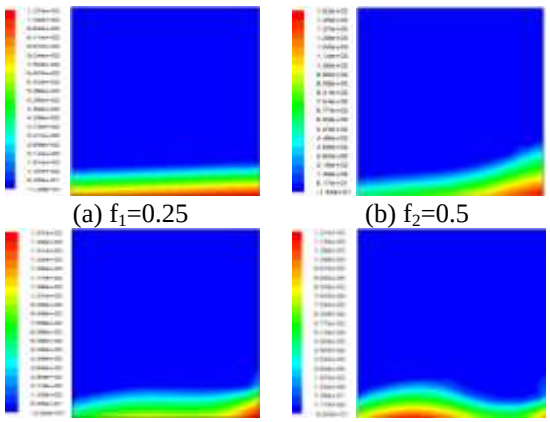

(a) f_1=0.25 (b) f_2=0.5

(c) f_3=0.79 (d) f_4=0.9

Fig. 16 Distribution of static pressure at t=3T/4.

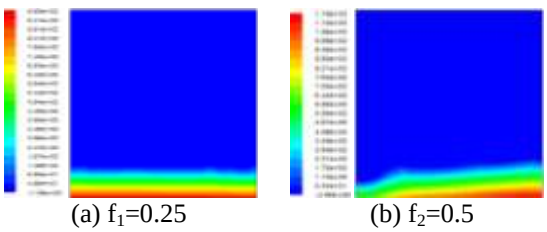

(a) f_1=0.25 (b) f_2=0.5

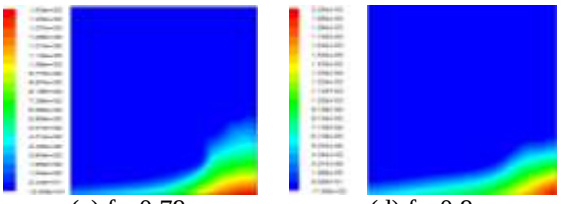

(c) f_3=0.79 (d) f_4=0.9

Fig. 17 Distribution of static pressure at t=T.

4.5 Dynamic pressure

The distribution of the dynamic pressure in the tank for the considered values of frequency is presented in figures 18, 19, 20 and 21. From these results, it is clear that the dynamic pressure distribution depends significantly on the external excitation frequency. In fact, the maximum value of the dynamic pressure is observed for the maximum value of the frequency for t=T/4, t=T/2 and t=3T/4. However, the minimum value is obtained for the minimum value of frequency. At t=T, the maximum value has been noted for f_3=0.79 Hz. Also, the location of the maximum value in the tank varied with motion of the liquid in the tank. In addition, we note that the maximum value of the dynamic pressure appears in the recirculation zones.

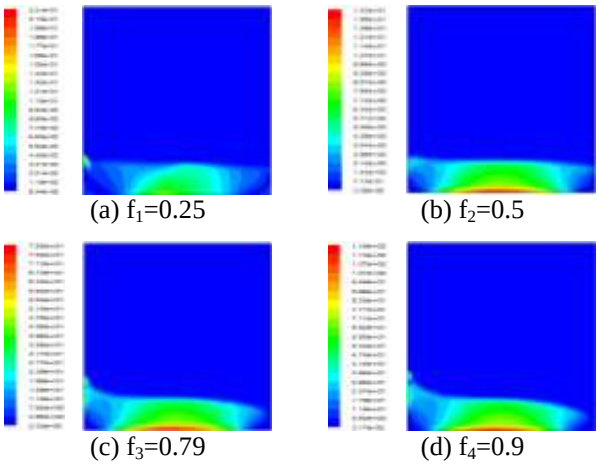

(a) f_1=0.25 (b) f_2=0.5

(c) f_3=0.79 (d) f_4=0.9

Fig. 18 Distribution of Dynamics pressure at. t=T/4.

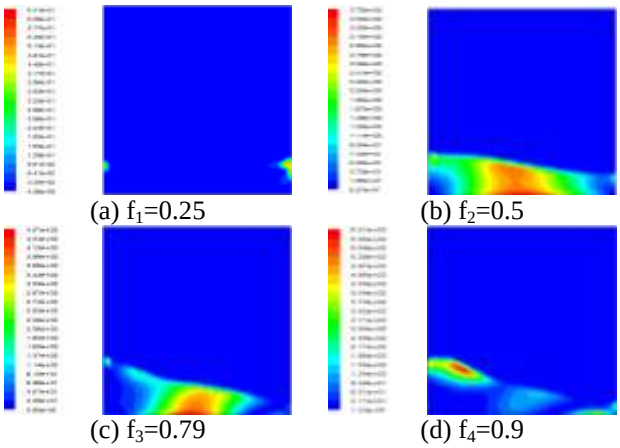

(a) f_1=0.25 (b) f_2=0.5

(c) f_3=0.79 (d) f_4=0.9

Fig. 19 Distribution of Dynamics pressure at t=T/2.

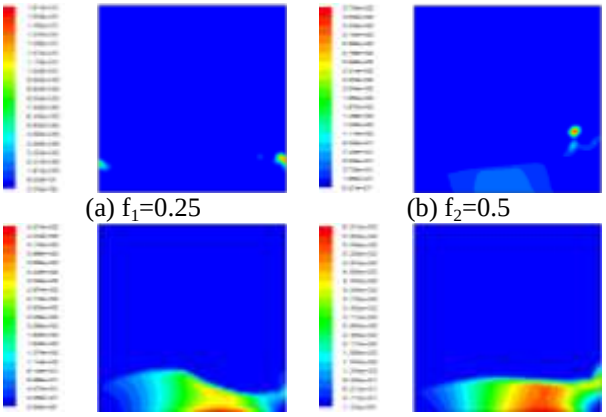

(a) f_1=0.25 (b) f_2=0.5

(c) f_3=0.79 (d) f_4=0.9

Fig. 20 Distribution of dynamic pressure at t=3T/4.

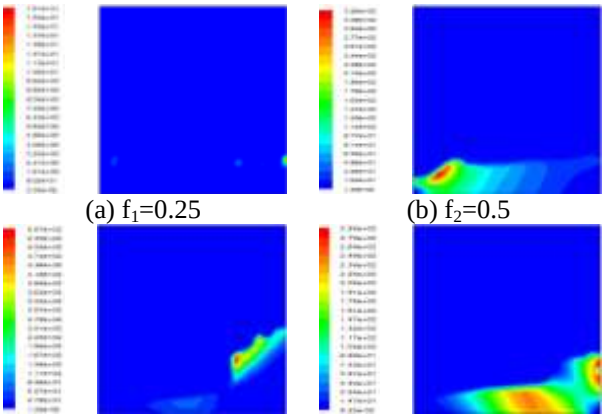

(a) f_1=0.25 (b) f_2=0.5

(c) f_3=0.79 (d) f_4=0.9

Fig. 21 Distribution of dynamic pressure at t=T.

5 Comparison with experimental results

Figure 22 shows the variation of the static pressure for the different values considered in this study. Particularly, we compare our numerical results with the experimental results of Panigrahy et al. [22] for the case of the frequency equal to f_1=0.25 Hz. The comparison gives a good agreement which confirm the validity of our numerical model. Such results indicate that the variation of the pressure is characterized by a sinusoidal behavior for the different values of frequency. In the other hand, we note that the period of the pressure varied with the variation of the frequency. In fact, it increases with the decrease of the frequency value. The maximum value of the pressure is observed for f_4=0.9 Hz and the minimum value is obtained for f_1=0.25 Hz. For the natural frequency equal to f_3=0.79 Hz and the frequency f_4=0.9 Hz, it has been noted that the value of the static pressure are very close.

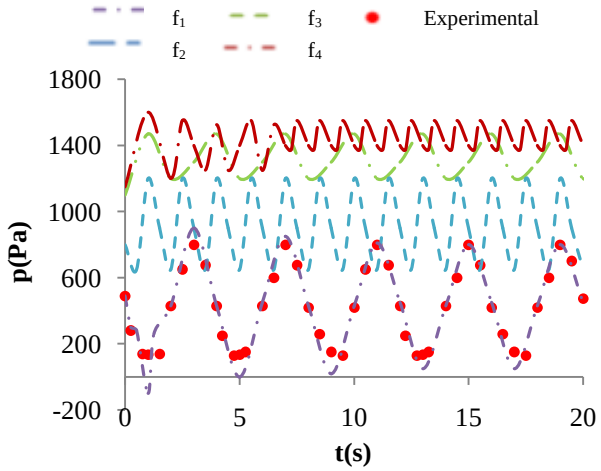

Fig. 24 Static pressure profile

6 Conclusion

In this paper, we studied the liquid sloshing phenomena in a rectangular tank subjected to an external excitation. The VOF method is used to predict the free surface evolution over time. Particularly, the effect of the external excitation frequency is investigated. In fact, four different values of frequency are examined. The results show that the sloshing phenomena depend strongly on the frequency value. Indeed, all numerical parameters are affected by the frequency value. The free surface evolution becomes more important with the increase of the external excitation frequency. The liquid moves slowly for a weak value of frequency, whereas the liquid sloshing becomes more violent with the increase of the frequency. For the velocity, we conclude that the recirculation zones become more important with the increase of the frequency. Also, the velocity value increase with the increase of the external excitation frequency. The same conclusion can be drawn for the static and the dynamic pressure. The results are affected strongly by the value of movement frequency. In fact, the location of the compression zones on the tank depends on the frequency values. From these results, we conclude that the sloshing phenomena in the rigid tank depend on the external excitation parameters, especially on the frequency for an external sinusoidal excitation.
An interesting perspective is to develop an experimental setup to study the liquid sloshing in other representative cases. Further work in this context is in progress.

References:

[1] Akyildiz, H., Unal, N. E., Experimental investigation of pressure distribution on a rectangular tank due to the liquid sloshing. *Ocean Engineering*, 32, 2005, 1503-1516.

[2] Molin, B., Remy, F., Experimental and numerical study of the sloshing motion in a rectangular tank with a perforated screen. *Journal of Fluids and Structures*, 43, 2013, 463-480

[3] Jin, H., Liu, Y., Li, J. H., Experimental study on sloshing in a tank with an inner horizontal perforated plate, *Ocean Engineering*, 82, 2014, 75-84

[4] Yan, G., Rakheja, S., Siddiqui, K., Experimental study of liquid slosh dynamics in a partially filled tank, *Journal of Fluids Engineering*, 7, 2009, 131-145

[5] Goudarzi, M. A., Sabbagh-Yazdi, S. R., Investigation of nonlinear sloshing effects in seismically excited tanks, *Soil Dynamics and Earthquake Engineering*, 43, 2012, 355–365.

[6] Koh, C. G., Luo, M., Gao, M., Bai, W. Modelling of liquid sloshing with constrained floating baffle, Computers and Structures, 122, 2013, 270-279

[7] Ji, Y. M., Shi, Y. S., Park, J. S., Hyun, J. M. Experiments on non-resonant sloshing in a rectangular tank with large amplitude lateral oscillation, *Ocean Engineering*, 50, 2012, 10–22

[8] Jung, J. H., Yoon, H. S., Lee, C.Y., Shin, S. C., Effect of the vertical baffle height on the liquid sloshing in a three-dimensional rectangular tank, *Ocean Engineering*, 44, 2012, 79-89

[9] Hou, L., Li, F., A Numerical Study of Liquid Sloshing in a Two-dimensional Tank under External Excitations, *Journal of Marine Science and Application*, 11, 2012, 305-310.

[10] Akyıldız, H., Unal, N. E., Aksoy, H., An experimental investigation of the effects of the ring baffles on liquid sloshing in a rigid cylindrical tank, *Ocean Engineering*, 59, 2013, 190-197.

[11] Meziani, B., Ourrad, O., Capillary effect on the sloshing of a fluid in a rectangular tank submitted to sinusoidal vertical dynamical excitation, *Journal of hydrodynamics* 26: 2014, 326-338

[12] Navid, N. N., Mahmood, F. G., Numerical simulation of filling process of natural gas onboard vehicle cylinder. *Journal of the Brazilian Society of Mechanical Sciences and Engineering*, 2012, DOI 10.1007/s40430-013-0098-7

[13] Dilson, J. S. Walter L. W., Rolf Bertrand Schroeter, Cleiton Rodrigues Teixeira, Influence of the cutting edge micro-geometry of PCBN tools on the flank wear in orthogonal

quenched and tempered turning M2 steel, *Journal of the Brazilian Society of Mechanical Sciences and Engineering*, 2013, DOI 10.1007/s40430-013-0116-9

[14] Alexandre, M. W., Reyolando, M. B., Jose´ M. B., The first frequency of cantilevered bars with geometric effect: a mathematical and experimental evaluation, *Journal of the Brazilian Society of Mechanical Sciences and Engineering*, 2013, 35, 457–467

[15] Elmer, M. G., Leandro, G. S., Vinicius, M., Danilo, C. R., Marcello, A. M. Verification and accuracy comparison of commercial CFD codes using hydrodynamic instability, *Journal of the Brazilian Society of Mechanical Sciences and Engineering*, 2013, 36, 59-68

[16] Yu, Y., Shademan, M., Barron, R. M., Balachandar, R., CFD study of effects of geometries variations on flow in a nozzle, *Engineering applications of computational fluid mechanics*, 6, 2012, 412-425

[17] Andersson, A. G., Andersson, P., Landström, T. S. CFD modeling and validation of free surface flow during spilling of reservoir in down scale model, *Engineering applications of computational fluid mechanics*, 7, 2013, 159-167

[18] Mnasri, C., Hafsia, Z., Omri, M., Maalel, K., A moving grid model for simulation of free surface behavior induced by horizontal cylinders exit and entry, *Engineering Applications of Computational Fluid Mechanics* 4, 2010, 260-275

[19] Sriram, V., Sannasiraj, S. A., Sundar, V., Numerical simulation of 2D sloshing waves due to horizontal and vertical random excitation, *Applied Ocean Research*, 28, 2006, 19-32.

[20] Godderidge, B., Turnock, S., Tan, M., Earl, C., An investigation of multiphase CFD modeling of a lateral sloshing tank, *Computers & Fluids*, 38, 2009, 183-193

[21] Bouabidi, A., Driss, Z., Abid, M. S., Vertical Baffles Height Effect on Liquid Sloshing in an Accelerating Rectangular Tank, *International Journal of Mechanics and Applications*, 3, 2013, 105-11.

[22] Panigrahy, P. K., Saha, P. K., Maity, U. K., Experimental studies on sloshing behavior due to horizontal movement of liquids in baffled tanks, *Ocean Engineering*, 36, 2009, 213-222

[23] Akyildiz, H., Unal, N. E., Sloshing in a three-dimensional rectangular tank: numerical simulation and experimental validation, *Ocean Engineering*, 33, 2006, 2135-2149.

[24] Driss, Z., Bouzgarrou, G., Chtourou, W., Kchaou, H., Abid, M. S., Computational studies of the pitched blade turbines design effect on the stirred tank flow characteristics, *European Journal of Mechanics B/Fluids*, 29, 2010, 236-245.

[25] Driss, Z., Mlayeh, O., Driss, D., Maaloul M, Abid, M. S., Numerical simulation and experimental validation of the turbulent flow around a small incurved Savonius wind rotor, *Energy*, 74, 2014, 506-517